MULTI-DIMENSIONAL CHARACTERIZATION OF MINERAL ABUNDACE IN ORDINARY CHONDRITE METEORITES. M. E. Gemma[1,2,3] (mgemma@ldeo.columbia.edu), D. S. Ebel[2,1,3], [1]Department of Earth and Environmental Science, Columbia University, New York, NY, 10027, [2]Department of Earth and Planetary Sciences, American Museum of Natural History (AMNH), New York, NY, 10024, [3]Lamont-Doherty Earth Observatory, Columbia University, Palisades, NY 10964.

Introduction: Mineralogy within ordinary chondrite meteorites is highly variable, dependent on petrologic type [1], and the result of differing parent body processes [2]. Quantifying representative mineralogy in meteorites often involves destructive processes [3, 4] which sacrifice petrographic context in the sample. Additionally, traditional methods such as point counting do not provide a realistic estimation of modal mineralogy in these ordinary chondrite samples due to their fine-grained nature.

We have combined the non-destructive methods of 3D computed tomography (CT) with 2D X-ray element intensity mapping of surfaces to quantitatively determine mineral modal abundances and variability across petrologic types of ordinary chondrite meteorites without losing petrographic context in each sample. This work is part of a broader effort to utilize precise mineral abundances in meteorites to quantitatively link laboratory spectroscopy of meteorites to spectroscopy of asteroids to better understand parent body and asteroid compositions.

Sample Selection: A total of 20 ordinary chondrite falls spanning the full range of petrologic types were sourced from the American Museum of Natural History meteorite collection: Nine LL chondrites [Semarkona (LL3.0), Parnallee (LL3.6), Savtschenskoje (LL4), Soko-Banja (LL4), Tuxtuac (LL5), Olivenza (LL5), Ensisheim (LL6), Mangwendi (LL6), and Kilabo (LL6)], eight L chondrites [Hallingeberg (L3.4), Khohar (L3.6), Tennasilm (L4), Bjurbole (L4), Mount Tazerzait (L5), Homestead (L5), Suizhou (L6), and Holbrook (L6)], and three H chondrites [Buzzards Coulee (H4), Jilin (H5), and Zhovtnevyi (H6)].

Methods: All samples were first scanned using AMNH's GE phoenix v|tome|x s240 computed tomography scanner to characterize their 3D structure and determine the abundance of opaque (metal and sulfide) phases in approximately 2-6 cm^3 volumes, with resolutions ranging from 6-11 microns/voxel. The CT data was reconstructed using phoenix datos|x software to render and process the 3D scan. Next, using VGstudio software, we were able to calculate the total volume of the sample, isolate mineral phases based on density, and calculate the volume of the metal and sulfide phases respectively (**Fig. 1**). Each sample was then cut and polished to create a thick or thin section of the meteorite. These sections were subsequently mapped using AMNH's Cameca SX100 Electron Microprobe for the X-ray intensities of ten major and minor elements (Mg, Si, Ca, Al, Fe, Ni, S, Ti, Cr, and P) at resolutions of 4-6 microns/pixel, over a sufficient area (~1 cm^2) to characterize mineralogy in a 2D slice (**Fig. 2**, *left*). Red-Green-Blue (RGB) composite images, using one element map in each color channel (Red = Mg, Green = Ca, Blue = Al), were used to qualitatively evaluate mineral diversity (**Fig. 2,** *right*).

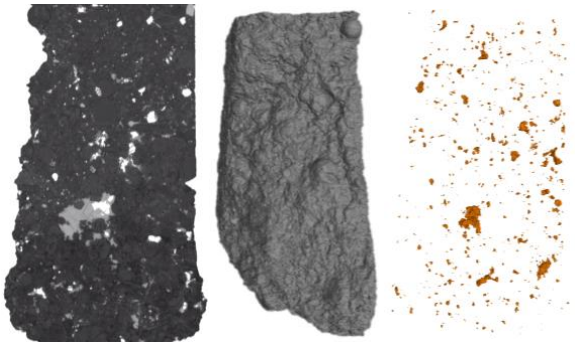

Figure 1: *Left*: 2D slice from 3D CT scan of Soko-Banja (LL4). Resolution = 8.8 microns/voxel. Major mineral phases in order of decreasing brightness: Metal, Sulfide, Pyroxene, Olivine. *Middle*: 3D volume rendered from tiff stack of X-ray maps from the CT scan. Total volume = 4.13 cm^3. Intact chondrule visible on upper right. *Right*: Metal inclusions segmented from 3D volume of Soko-Banja. Once desired mineral phase is isolated, phase abundance in the total volume can be calculated.

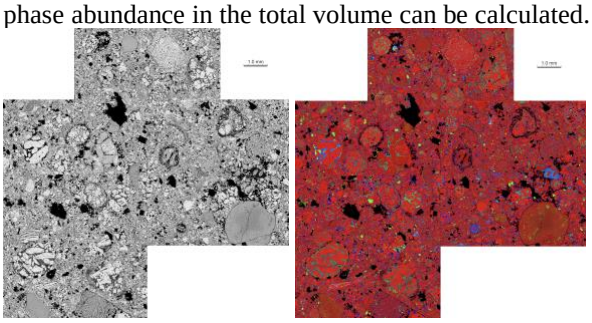

Figure 2: *Left*: X-ray element intensity map of Mg in thick polished section of Soko-Banja (LL4). Brighter areas represent higher abundances of Mg. *Right*: RGB composite image of mapped Soko-Banja section. Red = Mg, Green = Ca, Blue = Al. Area = 0.92 cm x 1.22 cm.

To quantitatively address mineral diversity, the acquired element maps were linearly combined to determine the mineralogy of each individual pixel in a map. This enabled calculation of the relative mineral abundances in each meteorite [5] (**Fig. 3, Table 1**). Metal and sulfide abundances determined from a 3D data can be used as a check against the 2D modal abundance map (**Fig. 3**) to ensure that the 2D section is representative.

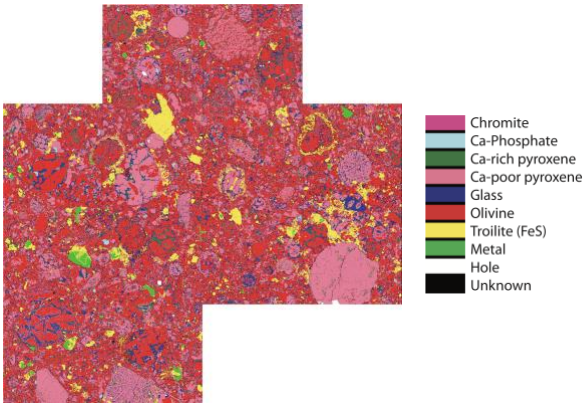

Figure 3: Mineral modal abundance map of Soko-Banja (LL4). Each pixel was assigned a mineral phase using linear combinations of the element maps. Area = 0.92 cm x 1.22 cm.

Mineral Phase	Parnallee (LL3.6)	Soko-Banja (LL4)	Tuxtuac (LL5)	Mangwendi (LL6)
Olivine	44.48%	40.96%	40.65%	46.87%
Ca-poor pyroxene	20.28%	29.32%	18.78%	21.8%
Glass	6.73%	9.70%	9.72%	10.14%
Ca-rich pyroxene	8.98%	3.36%	11.89%	5.09%
Troilite	5.19%	5.89%	6.14%	4.59%
Ca-phosphate	0.30%	0.38%	0.08%	0.42%
Kamacite	1.07%	N/A	0.03%	N/A
Taenite	0.65%	N/A	0.77%	N/A
Chromite	0.25%	0.16%	0.60%	0.35%
Metal	(1.72%)	0.82%	(0.8%)	0.50%
Unknown	12.04%	9.74%	11.32%	10.06%

Table 1: Mineral Modal Abundances of LL Chondrite samples from each petrologic type (3-6). Kamacite and Taenite values for Soko-Banja and Mangwendi were not calculated because Ni was not mapped. The metal values in parentheses for Parnallee and Tuxtuac are the values for Kamacite and Taenite added together (equivalent to the metal phase for Soko-Banja and Mangwendi).

Results/Discussion: 2D element mapping of a ~1 cm^2 sample surface area produces mineral abundances consistent with 3D bulk scans of a ~4 cm^3 parent sample (Fig. 5). Abundances of mineral phases in 2D and 3D are consistent to within 1% for equilibrated samples (petrologic types 4-6), and generally to within ~2% for the unequilibrated samples (petrologic type 3). The larger inconsistencies observed in the 2D and 3D abundances for the unequilibrated samples are likely due to the more heterogeneous nature of the unequilibrated meteorites (**Fig. 4**). Next steps include mapping multiple sections from a single unequilibrated ordinary chondrite to evaluate the effects of heterogeneity (or lack thereof) on 2D vs. 3D abundances. The calculated mineral modal abundances demonstrate that 2D mapping of an area ~0.6 cm^2 - 1 cm^2 is representative of the bulk meteorite sample. Calculated mineral abundances are also consistent with existing literature on the compositions of ordinary chondrites [3,4,6,7]. Olivine and Ca-poor pyroxene are the most modally dominant phases, followed by Ca-rich pyroxene, "glass" (~plagioclase), sulfide, and metal.

This method produces more precise mineral abundances (characterization at the ~micron scale) than point counting and preserves petrographic context of the sample (unlike powder X-Ray Diffraction). This work is not only useful as a non-destructive method that

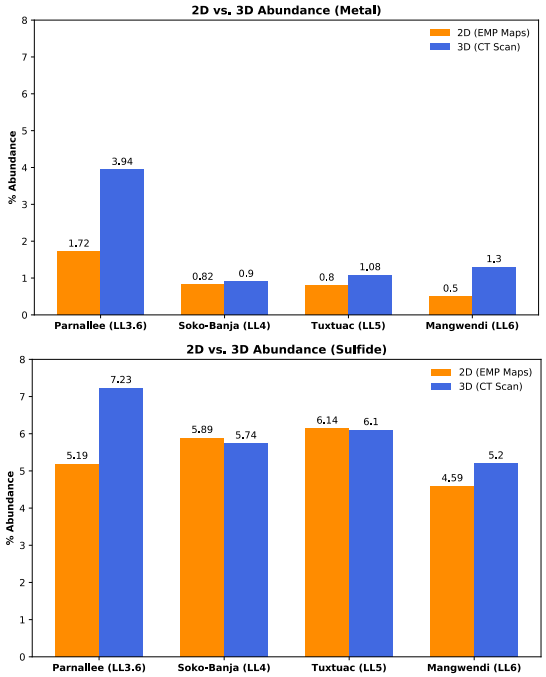

Figure 4: Comparison of metal (top) and sulfide (bottom) abundances in 2D vs. 3D.

preserves petrographic context, but also can be used to characterize laboratory spectroscopic measurements of the meteorite samples (concurrent work) and help remotely decipher parent-body asteroids.

Acknowledgements: The authors thank Henry Towbin and the staff at the AMNH Microscopy and Imaging and EPMA facilities for operation and analysis assistance. This work was supported by NASA Emerging Worlds grant NNX16AD37G (DE).

References: [1] McSween H. et al. (1991) Icarus, **90**, 107–116. [2] Jones R. H., et al. (2014) Geochim. Cosmochim. Acta **132**, 120–140. [3] Dunn T. et al. (2010) Meteor. Planet. Sci. **45**, 123-134. [4] Menzies O. et al. (2005) Meteor. Planet. Sci. **40**, 1023-1042. [5] Crapster-Pregont and Ebel (in press) Microscopy and Microanalysis. 1-13. [6] Gastineau-Lyons H. et al. (2002) Meteor. Planet. Sci. **37**, 75-89. [7] Weisberg M. et al. (2006) Meteorites and the Early Solar System, 19-52.